



저작자표시-비영리-변경금지 2.0 대한민국

이용자는 아래의 조건을 따르는 경우에 한하여 자유롭게

- 이 저작물을 복제, 배포, 전송, 전시, 공연 및 방송할 수 있습니다.

다음과 같은 조건을 따라야 합니다:



저작자표시. 귀하는 원저작자를 표시하여야 합니다.



비영리. 귀하는 이 저작물을 영리 목적으로 이용할 수 없습니다.



변경금지. 귀하는 이 저작물을 개작, 변형 또는 가공할 수 없습니다.

- 귀하는, 이 저작물의 재이용이나 배포의 경우, 이 저작물에 적용된 이용허락조건을 명확하게 나타내어야 합니다.
- 저작권자로부터 별도의 허가를 받으면 이러한 조건들은 적용되지 않습니다.

저작권법에 따른 이용자의 권리는 위의 내용에 의하여 영향을 받지 않습니다.

이것은 [이용허락규약\(Legal Code\)](#)을 이해하기 쉽게 요약한 것입니다.

[Disclaimer](#)

3D-FSE-Cube imaging without fat
suppression of the knee joint:
Optimization of scan parameters and
diagnostic accuracy comparison with
fat suppressed imaging at 1.5T MRI

Hee Woo Cho

Department of Medicine

The Graduate School, Yonsei University

3D-FSE-Cube imaging without fat
suppression of the knee joint:
Optimization of scan parameters and
diagnostic accuracy comparison with
fat suppressed imaging at 1.5T MRI

Directed by Professor Jin-Suck Suh

The Doctoral Dissertation
submitted to the Department of Medicine

The Graduate School of Yonsei University
in partial fulfillment of the requirements for the degree
of Doctor of Philosophy

Hee Woo Cho

June 2016

This certifies that the Doctoral
Dissertation of Hee Woo Cho is
approved.

Thesis Supervisor: Jin-Suck Suh

Thesis Committee Member #1: Young Han Lee

Thesis Committee Member #2: Doo Hoe Ha

Thesis Committee Member #3: Dong-Hyun Kim

Thesis Committee Member #4: Kwan Kyu Park

The Graduate School
Yonsei University

June 2016

ACKNOWLEDGEMENTS

First of all, I cannot express enough thanks to the thesis supervisor, Prof. Jin-Suck Suh who directed my graduate work with generosity from planning to completion, and to Prof. Young Han Lee who was an irreplaceable consultant for me – I must express my heartfelt thanks to you for being with me all times.

To Prof. Doo Hoe Ha; Prof. Dong-Hyun Kim; Prof. Kwan Kyu Park – Thank you very much for consistent encouragement and advice during the process of the doctoral dissertation.

And I would like to thank Prof. Hyung-Sik Kim for making a phantom and compiling surgical results. To Prof. Seok Hahn – Thank you for reviewing images with me for many hours. My work could not have happened without these helpers.

I would like to thank the radiology technicians of Yongin Severance Hospital including Yong Soo Shin who helped me perform MRI scans practically. And I also would like to thank staffs of the data processing department, Un Hyung Ryu and Hwa Sung Ahn who helped me on data documentation.

To the hospital director, Prof. Jin-Oh Park and the head

professor of the radiology, Prof. Soo Yoon Chung, in Yongin Severance Hospital – Thank you very much for helping me in many ways so that I could focus on research comfortably during the long course of this study.

To my parents and parents-in-law, I cannot express the depth of my gratitude in words. Finally, to my loving and supportive wife, Kyoung Mi and my little son, Yeon Joon – My deepest gratitude. The support of my family was the greatest encouragement to me.

<TABLE OF CONTENTS>

ABSTRACT	1
I. INTRODUCTION	5
II. MATERIALS AND METHODS	8
1. Phantom imaging	8
2. Subjective image evaluation	10
3. Objective image evaluation	11
4. Selection of optimized parameters from phantom imaging	11
5. Volunteer imaging and selection of optimized parameters	11
6. Imaging of patients	12
7. Review of patient imaging	14
8. Statistical analysis	15
III. RESULTS	16
1. Interpretation of phantom imaging	16
2. Interpretation of volunteer imaging	18
3. Interpretation of patient imaging	20
IV. DISCUSSION	24
V. CONCLUSION	34
REFERENCES	35
ABSTRACT (IN KOREAN)	40

LIST OF FIGURES

Figure 1. Subjective scores and signal-to-noise ratios (SNR) per unit time of phantom imaging	17
Figure 2. 3D-FSE-Cube images of porcine knee phantom ..	18
Figure 3. Scan time of 3D-FSE-Cube in volunteer imaging	19
Figure 4. SNR per unit time of volunteer imaging	20
Figure 5. Medial collateral ligament tear in 3D-FSE-Cube imaging	28
Figure 6. False-positive subchondral bone marrow edema (BME) lesion on 3D-FSE-Cube without fat suppression (NFS).....	29
Figure 7. Reduced metal artifact on 3D-FSE-Cube-NFS	31
Figure 8. 3D-FSE-Cube-NFS for replacing inappropriate 3D-FSE-Cube with fat suppression (FS)	32
Figure 9. 3D-FSE-Cube-NFS for detecting subtle BME lesions	32

LIST OF TABLES

Table 1. Parameter settings in phantom imaging	9
Table 2. Parameter settings in patient imaging	13
Table 3. Diagnostic performance of 3D-FSE-Cube-FS and 3D-FSE-Cube-NFS for the detection of knee joint lesions ..	22

Table 4. Sensitivity and Specificity of 3D-FSE-Cube-FS and 3D-FSE-Cube-NFS for the detection of cartilage lesions ...	23
Table 5. Interobserver agreement rates with unweighted kappa	24

ABSTRACT

**3D-FSE-Cube imaging without fat suppression of the knee joint:
Optimization of scan parameters and diagnostic accuracy
comparison with fat suppressed imaging at 1.5T MRI**

Hee Woo Cho

*Department of Medicine
The Graduate School, Yonsei University*

(Directed by Professor Jin-Suck Suh)

Background and Purpose: Three-dimensional fast spin-echo imaging sequence with variable flip angle (3D-FSE-Cube) images have been developed recently and established as an essential sequence in the routine knee magnetic resonance imaging (MRI) protocol. However, no study has compared 3D-FSE-Cube imaging of the knee joints “with” and “without” fat suppression, and the diagnostic performance of 3D-FSE-Cube imaging without fat suppression (3D-FSE-Cube-NFS) has not yet been investigated. The aims of this study were as follows: (1) to optimize scan parameters for 3D-FSE-Cube imaging with fat suppression (3D-FSE-Cube-FS) and

3D-FSE-Cube-NFS in 1.5T knee MRI and (2) to compare 3D-FSE-Cube-FS and 3D-FSE-Cube-NFS to evaluate the diagnostic performance of 3D-FSE-Cube-NFS for detecting lesions of the meniscus, ligaments, bone marrow, or cartilage in knee imaging.

Materials and Methods: A porcine knee phantom was used to optimize scan parameters for 3D-FSE-Cube imaging both with and without fat suppression in a 1.5T MRI system (Signa Horizon; GE Healthcare, Waukesha, WI, USA). Sagittal images with varied settings of repetition time (TR) from 1000 to 1300 ms and echo train length (ETL) from 30 to 60 were acquired. The image acquired with TR=1300 ms and ETL=30 served as a reference scan. Two musculoskeletal radiologists graded all images on a scale from -8 to 8 on the basis of image blurring and overall image quality relative to the reference scan. Subsequently, the same survey was performed on a healthy human volunteer by using parameter settings that received scores of -2 or above in the phantom study. Images with a score of -1 or above were regarded as acceptable. Signal-to-noise ratio (SNR) and SNR per unit time were measured in the patellar cartilage and femoral bone marrow on each image. After consideration of both subjective image evaluation and SNR per unit time, optimized scan parameters were determined. Using these optimized parameters, knee

MRI scans were performed on 124 patients with knee pain by using both 3D-FSE-Cube-FS and 3D-FSE-Cube-NFS between September 2015 and December 2015. Among these patients, 25 subsequently underwent arthroscopic surgeries. Using the arthroscopic results and 2D images as reference standards, the two radiologists compared the diagnostic performance of 3D-FSE-Cube-NFS and 3D-FSE-Cube-FS images to determine which sequence was more diagnostically useful in a particular clinical situation, such as ligament tear, meniscus tear, subchondral bone marrow edema (BME) lesions, or cartilage defect. McNemar's test was performed to compare the diagnostic performance of the two sequences at a significance level of $p < 0.05$.

Results: Image quality and SNR increased with longer TR and shorter ETL. Among phantom images with a score of -1 or above, the highest SNR per unit time was acquired with scan parameters of TR=1300 ms and ETL=45 in both images with fat suppression (FS) and without fat suppression (NFS). In subsequent volunteer imaging, the same parameters were found to be the best with and without FS. In the imaging study of the 124 patients, there were no significant differences between the two sequences for the detection of meniscus tears and cartilage defect except for medial collateral ligament (MCL) tears and subchondral BME

lesions. Compared to 3D-FSE-Cube-FS, 3D-FSE-Cube-NFS had lower sensitivity for the detection of MCL tears, and lower sensitivity and specificity for the detection of BME lesions. Nevertheless, 3D-FSE-Cube-NFS images showed advantages, such as reduced susceptibility artifact, ability for replacing inappropriate 3D-FSE-Cube-FS images, and detection of subtle BME lesions.

Conclusion: Considering both acceptable image quality and short scan time, the optimized scan parameters for both 3D-FSE-Cube FS and 3D-FSE-Cube NFS were found to be TR=1300 ms and ETL=45. 3D-FSE-Cube-FS and 3D-FSE-Cube-NFS also showed similar sensitivity and specificity for the detection of meniscus tears or cartilage defect, except for the detection of MCL tears and detection of BME lesions. Additional 3D-FSE-Cube-NFS has considerable advantages such as reduced susceptibility artifact, which make it a suitable option for replacing inappropriate 3D-FSE-Cube-FS images in some clinical situations.

Key words: knee, magnetic resonance imaging, three-dimensional, fat suppression

**3D-FSE-Cube imaging without fat suppression of the knee joint:
Optimization of scan parameters and diagnostic accuracy
comparison with fat suppressed imaging at 1.5T MRI**

Hee Woo Cho

*Department of Medicine
The Graduate School, Yonsei University*

(Directed by Professor Jin-Suck Suh)

I. Introduction

Magnetic resonance imaging (MRI) is a widely used standard imaging technique for the diagnosis of abnormalities of bones, cartilages, ligaments, and menisci in the knee joints¹. While conventional MRI protocols include various planes of two-dimensional (2D) fast spin-echo (FSE) sequences, three-dimensional (3D) FSE imaging with variable flip angle (Cube) is isotropically acquired with thin sections and can be reconstructed in any plane

without image quality degradation. This 3D FSE imaging includes volume isotropic turbo spin-echo acquisition (VISTA[®]; Philips Healthcare, Best, the Netherlands), sampling perfection with application-optimized contrasts using different flip-angle evolution (SPACE[®]; Siemens Healthcare, Forchheim, Germany), and Cube[®] (GE Healthcare, Waukesha, WI, USA). 3D-FSE-Cube imaging has many advantages including high spatial resolution, reduced partial volume averaging, relatively shorter scan time, and possible multiplanar reformation¹⁻⁴. Moreover, recent studies have shown that 3D-FSE-Cube imaging has sensitivity, specificity, and accuracy comparable to conventional 2D FSE imaging in the comprehensive evaluation of knee joint injuries⁴⁻¹³. Therefore, 3D-FSE-Cube imaging is currently well established as an essential sequence in the routine knee MRI protocol at many institutions.

Most previous studies on 3D isotropic imaging were conducted mainly using 3.0T MRI rather than 1.5T MRI^{2-5,7,8,11,13,14}. However, a study has shown that 3D isotropic imaging in 1.5T knee MRI also has a similar or superior diagnostic performance compared to conventional 2D imaging⁹.

A volunteer imaging study was recently conducted for the optimization of scan parameters in a 3.0T knee MRI¹⁵. By optimizing scan parameters, the

authors could increase overall image quality and decrease image blurring¹⁵. In addition, scan parameter optimization is needed to solve the practical problem of a longer scan time resulting from the additional scan performed during 3D-FSE-Cube imaging without fat suppression (NFS). However, to my knowledge, no study has been published on scan parameter optimization of 3D isotropic imaging with a 1.5T MRI system.

I also paid attention to 3D isotropic NFS imaging as a challenging topic. The fat saturation technique for fat signal suppression routinely applied by 3D-FSE-Cube imaging in knee MRI has disadvantages over imaging without fat suppression, e.g., the presence of relatively more severe susceptibility artifacts¹⁶. Furthermore, a recent comparative study showed that 3D isotropic NFS imaging is significantly more superior to the routine fat suppressed (FS) imaging for ligament traceability in ankle MRI¹⁷. These suggest the possibility that 3D isotropic NFS imaging in knee MRI might be more helpful than FS imaging for the evaluation of ligaments or other structures of the knee joint with reduced susceptibility artifact and better ligament traceability under certain clinical situations. Therefore, studies comparing the overall diagnostic performances of 3D-FSE-Cube-NFS with 3D-FSE-Cube-FS for knee joint lesions are

desperately needed at this point. To the best of my knowledge, no study has compared isotropic 3D-FSE-Cube imaging of the knee joint “with” and “without” fat suppression, and no study has investigated the diagnostic performance of 3D-FSE-Cube-NFS.

The purposes of this study were as follows: (1) to optimize scan parameters for 3D-FSE-Cube-FS and 3D-FSE-Cube-NFS in 1.5T knee MRI and (2) to compare 3D-FSE-Cube-NFS and 3D-FSE-Cube-FS to evaluate the diagnostic performance of 3D-FSE-Cube-NFS for detecting knee lesions in the meniscus, ligaments, bone marrow, or cartilage.

II. Materials and Methods

Phantom imaging

A freshly harvested porcine knee phantom was imaged using a 1.5T MRI system (Signa Horizon; GE Healthcare, Waukesha, WI, USA) with an 8-Channel HD transmitter/receiver knee array coil (GE Healthcare). MRI scans with varying parameter settings of repetition time (TR) and echo train length (ETL) were acquired. At first, the phantom was subjected to sagittal 3D-FSE-Cube-FS and sagittal 3D-FSE-Cube-NFS by using parameters of TR=1300 ms and ETL=30. A fat suppression technique using

frequency-selective radiofrequency pulse was applied for 3D-FSE-Cube-FS. These scans served as a reference for subjective image quality assessment of the other scans. Ranges of the parameters used are shown in Table 1.

Table 1. Acquisition parameter settings for the reference scan and parameters for all other scans in the phantom study using 3D-FSE-Cube imaging with 1.5T MRI

Parameter	Reference	Ranges			
		Minimum		Maximum	
TR (ms)	1300	1000	1100	1200	1300
ETL	30	30		45	60
rBW (kHz)	50				
NEX	0.5				
ACC	1.74				
TE (ms)	30				
Matrix size	320 × 320				
FOV (mm)	160 × 160				
*Slice thickness (mm)	0.5				

Note 1: TR=repetition time; ETL=echo train length; rBW=receiver bandwidth; NEX=number of excitations; ACC=acceleration factor; TE=echo time; FOV=field of view

* 0.5-mm-slice-thickness isovoxel imaging was reformatted with interpolation after

1.6-mm–slice-thickness scanning

Number of excitations (NEX) and parallel imaging acceleration factor (ACC) were not changed because any change in these parameters would increase the 3D-FSE-Cube imaging scan time to more than 6 minutes, which is unacceptable in clinical imaging. Echo time (TE) was kept constant to maintain constant image contrast weighting in all scans. Slice thickness and number, matrix size, and field of view (FOV) were not changed to maintain constant voxel size. Receiver bandwidth (rBW) was also not changed because of image blurring and insufficient fat suppression.

Subjective image evaluation

The subjective image evaluation method was similar to a previously described method in a recent imaging optimization study¹⁴. All 3D-FSE-Cube scans were evaluated for image quality by two fellowship-trained musculoskeletal radiologists with 9 years of experience each. Readers evaluated each scan relative to the reference scan on an integer scale for image blurring and overall image quality. The score, which ranged from -2 to 2, corresponded with significantly worse, slightly worse, no difference (score of zero), slightly better, and significantly better than the reference score for each quality metric. The total score given by the two readers for each scan ranged from -8 to 8. Images with a score of -1 or above were regarded as acceptable.

Objective image evaluation

Signal-to-noise ratio (SNR) and SNR per unit time (minute) were measured in the patellar cartilage and femoral bone marrow on the sagittal image of each sequence as an objective measure of image quality. Regions of interest were placed in the center area of the lateral patellar cartilage and distal femoral epiphyseal bone marrow.

Selection of optimized parameters from phantom imaging

Selection of optimized scan parameters was performed in the following order: (1) higher image quality (score of 2 or above) than the reference scan on subjective evaluation, or (2) similar image quality (score of -1 or above) relative to the reference scan on subjective image evaluation and highest SNR per unit time.

Volunteer imaging and selection of optimized parameters

Because actual images acquired from patients may have parameters different from those of the phantom images, I performed additional in vivo volunteer imaging on a healthy 38-year-old woman. However, because the volunteer was a real human subject, the applied MRI scan parameters were limited to a score of -2 or above on the phantom images for a relatively shorter total scan time. Selection of optimized scan parameters was performed in a

manner identical to that used in the phantom imaging study.

Imaging of patients

After determining the optimized scan parameters based on phantom and volunteer in vivo imaging, knee MR imaging was performed on patients with knee pain by using a protocol, which comprised 2D FSE sequences, optimized 3D-FSE-Cube-FS, and optimized 3D-FSE-Cube-NFS sequences, between September 2015 and December 2015. Two of the 126 patients who underwent knee MRI during this period were excluded because of severe artifacts. The remaining 124 patients included 52 men and 72 women, with an age range of 11–91 years (mean, 46.1 years). 2D FSE sequences routinely included axial T1-weighted images, sagittal T2-weighted images, axial fat-suppressed T2-weighted images, and coronal fat-suppressed T2-weighted images. Details of the scan parameters are described in Table 2.

Table 2. Acquisition parameter settings for routine knee MRI of patients

Parameter	Sequence				Optimized
	Ax T1WI	Sag T2WI	Ax FS T2WI	Cor FS T2WI	3D-FSE-Cube-FS and optimized 3D-FSE-Cube-NFS
TR (ms)	533	4000	4600	4500	1300
TE (ms)	12	78	72	79	30
ETL	4	14	15	15	45
rBW (kHz)	31	31	35	35	50
NEX	1	2	2	2	0.5
Matrix size	256 x 256	480 x 256	288 x 256	480 x 256	320 x 320
FOV (mm)	150	160	150	160	160
Slice thickness (mm)	4	4	4	4	*0.5
Scan time (min)	1:56	2:48	2:52	2:47	3: 52 each

Note 1: TR=repitition time; TE=echo time; ETL=echo train length; rBW=receiver bandwidth;
 NEX=number of excitations; FOV=field of view; T1WI=T1-weighted imaging;
 T2WI=T2-weighted imaging

* 0.5-mm-slice-thickness isovoxel imaging was reformatted with interpolation after
 1.6-mm-slice-thickness scanning

The 3D-FSE-Cube sequences were obtained using a 2D auto-calibrating parallel imaging reconstruction technique (ARC; GE Healthcare). The 3D-FSE-Cube isotropic source data were used to create sagittal, coronal, and axial reformatted images of the knee joint. Image post-processing was

performed by a MRI technologist on the MR console (GE Healthcare) immediately after the MRI scan.

Review of patient imaging

All MR images were independently reviewed at a separate workstation by the two abovementioned readers, who were blinded to the radiologic reports of the knee MRI and results of the arthroscopic surgery.

At the first review session, the readers evaluated only the 3D-FSE-Cube-FS images of each patient for the presence or absence of ligament tear, meniscus tear, subchondral bone marrow edema (BME) lesions, and cartilage defect by using a picture archiving and communication system (PACS). At the second review session, the readers evaluated only the 3D-FSE-Cube-NFS images of each patient after 2 weeks to minimize recall and learning bias.

The arthroscopic surgical findings were regarded as a reference for cruciate ligament tear, meniscus tear, and cartilage defect. Arthroscopic surgeries were performed by an orthopedic surgeon with 17 years of experience. For medial collateral ligament (MCL) tear and BME lesions, the two readers established a reference in consensus by using all routine 2D and optimized 3D images with clinical information. A MCL tear was defined as a complete discontinuity or blurring of the ligament fibers, and a BME lesion was defined as a high signal intensity lesion on fat-suppressed T2-weighted images

involving the subchondral bone of the knee joint. Lateral collateral ligament (LCL) tear was not included in this study because of no patient involvement. For tears of the anterior cruciate ligament (ACL), posterior cruciate ligament (PCL), and MCL, a partial tear was also considered a true tear and was not distinguished from a complete tear. A meniscus tear was defined as increased intrameniscal signal intensity extending to the superior or inferior meniscal surface^{18,19}. Types of meniscus tears, such as vertical or radial tears, were not considered in this study. Specifying the location of the meniscus tear enabled comparison with the arthroscopic surgical report.

Cartilage defect was evaluated at each segment, including the medial femoral condyle, medial tibial plateau, lateral femoral condyle, lateral tibial plateau, patella, and femoral trochlea. The readers graded cartilage lesions by using a modified Noyes classification system (grade 0=normal cartilage; grade 1=increased T2 signal intensity of morphologically normal cartilage; grade 2A=superficial partial-thickness cartilage lesion < 50% of the total thickness of the articular surface; grade 2B=deep partial-thickness cartilage lesion > 50% of the total thickness of the articular surface; and grade 3=full-thickness cartilage lesion)²⁰⁻²³.

Statistical analysis

Interobserver agreement rates were tested by non-weighted kappa (k) statistics. A k-value of 0.0~0.20 indicated slight, 0.21~0.40 indicated fair,

0.41~0.60 indicated moderate, 0.61~0.80 indicated good, and 0.81~1.00 indicated excellent interobserver agreement²⁴. McNemar's test was used to determine any significant difference between the diagnostic performance of 3D-FSE-Cube-NFS and 3D-FSE-Cube-FS images for detection of knee lesions including ligament tears, meniscus tears, cartilage lesions, or BME lesions. A p-value less than 0.05 indicated statistical significance.

III. Results

Interpretation of phantom imaging

Results of evaluation of phantom imaging by readers are shown in Figure 1. Image quality and SNR increased with longer TR and shorter ETL; therefore, no images had more scores than the reference scan in subjective image evaluation. Three parameter settings each with acceptable image quality (score -1 or above) were noted in the FS (TR and ETL: 1200 ms and 30, 1200 ms and 45, and 1300 ms and 45) and NFS sequences (TR and ETL: 1100 ms and 30, 1200 ms and 30, and 1300 ms and 45), except for the reference scan. Among these settings including the reference scan, a parameter setting that showed the highest SNR per unit time was TR=1300 ms and ETL=45 in both the FS and NFS sequences (Fig. 1 and Fig. 2).

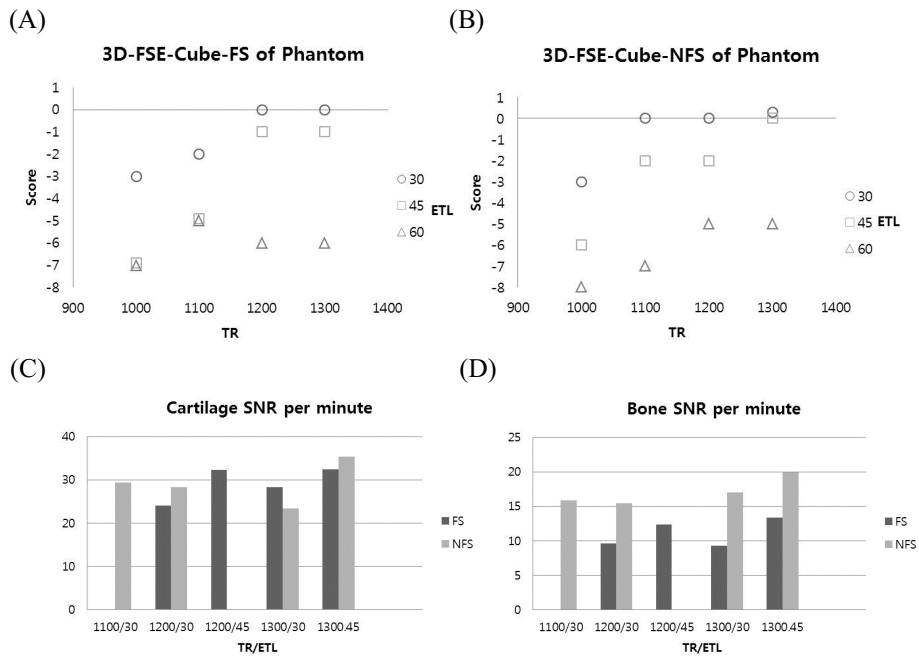


Figure 1. Subjective scores of phantom imaging with fat suppression (A) and without fat suppression (B). Images with a score of -1 or above were regarded as acceptable. The highest SNRs per unit time were acquired with scan parameters of TR=1300 ms and ETL=45 in both FS and NFS images with parameter settings of acceptable image quality, measuring in the patellar cartilage (C) and femoral epiphyseal bone marrow (D).

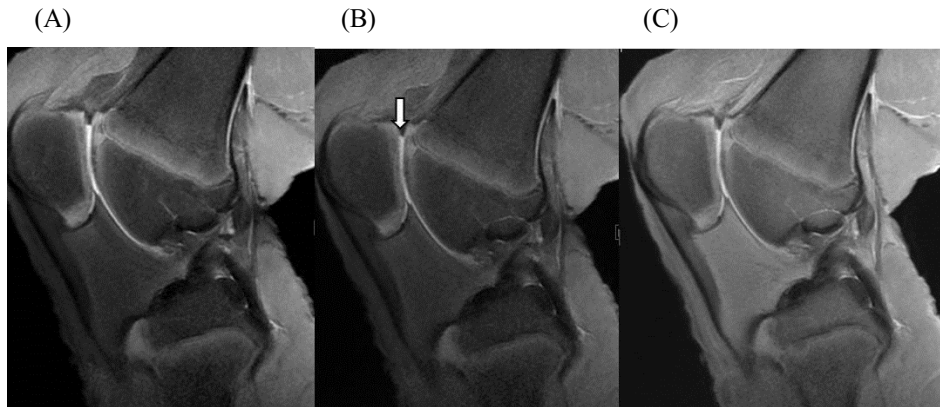


Figure 2. 3D-FSE-Cube images of porcine knee phantom. (A)

3D-FSE-Cube-FS image with optimized parameters, TR=1300 ms and ETL=45.

(B) 3D-FSE-Cube-FS image with TR=1000 ms and ETL=45. The total score given for this image by two readers was -7. Image blurring is visible at the patellofemoral joint (arrow). (C) 3D-FSE-Cube-NFS image with optimized parameters.

Interpretation of volunteer imaging

A 38-year-old healthy female volunteer underwent knee MRI with five FS sequences and six NFS sequences at a parameter setting that yielded scores of -2 or above in the subjective image evaluation of the phantom study. As a result, all sequences showed scores of acceptable image quality (score -1 or above). While only two FS sequences (TR and ETL: 1100 ms and 30, and 1200

ms and 45) had scores of -1, the other three FS sequences and all NFS sequences had scores of zero. Imaging at a shorter TR and longer ETL reduces scan time (Fig. 3). SNRs per unit time in the patellar cartilage and femoral epiphyseal bone marrow are shown in Figure 4. The sequence with the highest SNR per unit time had a parameter setting of TR=1300 ms and ETL=45 in both the FS and NFS images, which was identical to the results of the phantom study.

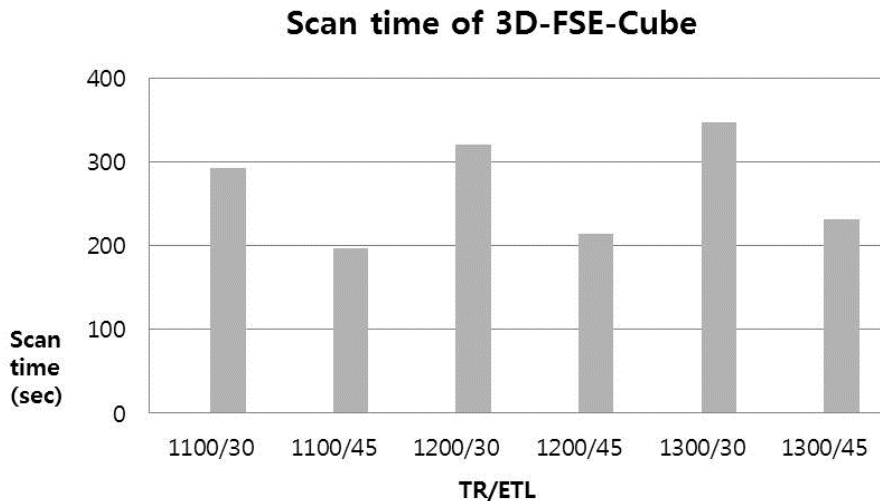


Figure 3. 3D-FSE-Cube scan time in volunteer imaging. Imaging at shorter TR and longer ETL reduces scan time. There is no difference in scan times between FS and NFS imaging.

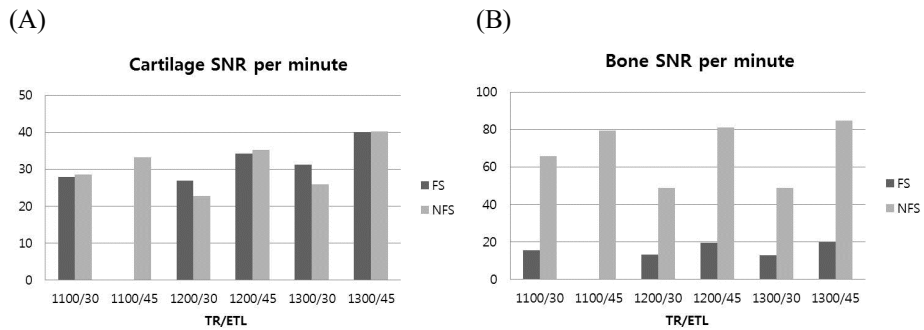


Figure 4. Signal-to-noise ratios (SNRs) per unit time of volunteer imaging measured in the patellar cartilage (A) and femoral epiphyseal bone marrow (B). FS images with TR=1100 ms and ETL=45 were not acquired in volunteer imaging because of a low score during the phantom study. Images with scan parameters of TR=1300 ms and ETL=45 showed the highest SNR per unit time at every setting.

Interpretation of patient imaging

The 25 arthroscopic surgeries revealed 3 ACL tears, 1 PCL tear, 17 medial meniscus (MM) tears, and 6 lateral meniscus (LM) tears. Moreover, 88 segments of cartilage defect were found among 150 segments of the 25 knee joints. There were no statistically significant differences between the 3D-FSE-Cube-NFS and 3D-FSE-Cube-FS sequences for the detection of meniscus tear and cartilage defect. Imaging of the 124 patients with knee pain showed that 3D-FSE-Cube-NFS had lower sensitivity for the detection of MCL

tear ($p < 0.001$) and lower sensitivity and specificity for the detection of subchondral BME lesions ($p < 0.001$), compared to 3D-FSE-Cube-FS (Table 3). Sensitivity and specificity of the sequences for the detection of cartilage defect lesions depending on their grades are shown in Table 4.

Interobserver agreement rates with unweighted kappa are presented in Table 5. Overall, 3D-FSE-Cube-NFS showed worse interobserver agreement than did 3D-FSE-Cube-FS. When assessing MM and LM tears, FS imaging showed excellent and good interobserver agreement, respectively, whereas NFS imaging showed moderate and fair interobserver agreement, respectively. For ACL tear or cartilage defect lesion, slightly better interobserver agreement rates were seen in FS imaging than in NFS imaging. For MCL tear, moderate interobserver agreement rate was seen in both FS and NFS imaging. However, for BME lesions, while moderate interobserver agreement was seen in FS imaging, only fair interobserver agreement was seen in NFS imaging.

Only fair interobserver agreement was seen both in FS and NFS imaging for the detection of cartilage defect lesions, which was relatively worse than the agreement for other knee lesions. This finding may be attributed to the difficulty in distinguishing cartilage defect grade 0 from grade 1 in those images. This can be explained by the result given in Table 4, which shows that sensitivity of the sequences for grade 1 cartilage defect lesion is much worse than that for high-grade lesions. Another reason was that one of the two reviewers was not familiar with 1.5T MRI images than those of 3.0T MRI. The relatively lower

diagnostic accuracy for cartilage defect lesion in this study can also be understood in the same context, as compared to the previous study⁹.

Table 3. Diagnostic performance of 3D-FSE-Cube-FS and 3D-FSE-Cube-NFS for the detection of knee joint lesions

Knee lesion	Sensitivity (%)		Specificity (%)		Accuracy (%)	
	Cube-FS	Cube-NFS	Cube-FS	Cube-NFS	Cube-FS	Cube-NFS
ACL tear (n=3/25)	66.7	66.7 [p=NA]	86.4	88.6 [p=0.564]	84.0	86.0
PCL tear (n=1/25)	0	50.0 [p=NA]	93.8	91.7 [p=NA]	90.0	90.0
MM tear (n=17/25)	94.1	85.3 [p=0.083]	81.3	75.0 [p=0.655]	90.0	82.0
LM tear (n=6/25)	100	83.3 [p=0.157]	79.0	73.7 [p=0.157]	84.0	76.0
Cartilage lesions (n=88/150)	75.6	75.0 [p=0.857]	43.6	34.7 [p=0.063]	62.3	58.3
MCL tear (n=16/124)	65.6	25.0 [p<0.001] *	97.7	93.1 [p=0.257]	93.6	89.5
BME lesions (n=205/744)	60.2	45.6 [p<0.001] *	98.3	94.3 [p<0.001] *	87.8	80.9

Note 1: 3D-FSE-Cube-FS=isotropic 3D-FSE imaging with fat suppression;

3D-FSE-Cube-NFS=isotropic 3D-FSE imaging without fat suppression; ACL=anterior cruciate ligament; PCL=posterior cruciate ligament; MM=medial meniscus; LM=lateral meniscus;

MCL=medial collateral ligament; BME=bone marrow edema

Note 2: Data represent combined data from the independent reviews of the two readers; data in brackets are p-values for the comparison of the two imaging techniques. NA means not applicable.

*p<0.05 indicates a significant difference.

Table 4. Sensitivity and Specificity of 3D-FSE-Cube-FS and 3D-FSE-Cube-NFS for the detection of cartilage lesions

Cartilage lesion (n=88)	Sensitivity (%)		Specificity (%)	
	FS	NFS	FS	NFS
Grade 1 (n=38)	59.2 [p=0.655]	61.8	43.6 [p=0.063]	34.7
Grade 2A (n=25)	82.0 [p=0.480]	78.0	43.6 [p=0.063]	34.7
Grade 2B (n=15)	96.7 [p=0.157]	90.0	43.6 [p=0.063]	34.7
Grade 3 (n=10)	85.0 [p=0.157]	95.0	43.6 [p=0.063]	34.7

Note 1: 3D-FSE-Cube-FS=isotropic 3D-FSE imaging with fat suppression;

3D-FSE-Cube-NFS=isotropic 3D-FSE imaging without fat suppression

Note 2: Data in brackets are p-values for the comparison of the two imaging techniques.

Table 5. Interobserver agreement rates with unweighted kappa

Knee lesion	3D-FSE-Cube-FS	3D-FSE-Cube-NFS
ACL tear (n=3)	0.750	0.595
MM tear (n=17)	0.905	0.403
LM tear (n=6)	0.675	0.371
Cartilage lesions (n=88)	0.264	0.213
MCL tear (n=16)	0.571	0.586
BME lesions (n=205)	0.508	0.301

Note 1: 3D-FSE-Cube-FS=isotropic 3D-FSE imaging with fat suppression;
 3D-FSE-Cube-NFS=isotropic 3D-FSE imaging without fat suppression; ACL=anterior cruciate
 ligament; MM=medial meniscus; LM=lateral meniscus; MCL=medial collateral ligament;
 BME=bone marrow edema

Data represent k-values

IV. Discussion

Recently, 3D-FSE-Cube imaging has almost always been included in the routine knee MRI protocol. Compared to consecutive multiple conventional 2D imaging, 3D-FSE-Cube imaging has a much shorter scan time and similar diagnostic performance. In recent years, many studies have compared the diagnostic performance of conventional 2D imaging and isotropic 3D FSE

imaging^{4,6-10}. However, although isotropic 3D FSE imaging can be implemented with a short scan time by using parallel imaging and a longer ETL, a single isotropic 3D FSE sequence has a relatively longer scan time than does a single 2D FSE sequence. In a previous study by Ai et al using a 1.5T MRI system, the mean scan time of 2D sequences was 2:30 but that of 3D-FSE-Cube sequence was 5:40⁹. A longer-than-usual scan time for a single sequence has many possible drawbacks, such as increased motion artifact, decreased patient comfort, decreased clinical efficiency, and burden of repeat scan.

The main purpose of this study was to compare the diagnostic performance of 3D-FSE-Cube-FS and NFS imaging sequences. The prior optimization study was designed to solve the problem of longer scan times because of the additional 3D-FSE-Cube-NFS scan. The results of this study show that imaging scan time could be remarkably decreased by using a shorter TR and longer ETL. However, extensive modification of the parameters for reducing scan time will significantly degrade image quality. The results of this study also revealed very poor image quality at a low TR of less than 1100 ms and long ETL of more than 60 during optimization. Therefore, obtaining optimized scan parameters is essential for balancing image quality and short scan time. Defining widely acceptable optimized scan parameters is difficult because radiologists might have differences of opinion on subjective image quality. A recent study that attempted to optimize knee MRI parameters for isotropic 3D-FSE imaging at 3.0T also failed to provide an appropriate one-scan

parameter setting¹⁵. Because no study has previously attempted to optimize scan parameters of isotropic 3D-FSE imaging even at 1.5T MRI, hospitals are forced to take their own approach to determine various scan parameter settings.

Because this study was performed under the actual clinical settings in my hospital, scan time for a routine knee MRI was limited. Because conventional 2D imaging sequences along the axial, sagittal, and coronal planes take a long time, the scan time of each 3D-FSE-Cube sequence was limited such that it did not exceed 6 minutes regardless of whether fat suppression was applied. Therefore, changes in TR and ETL had to be limited to the ranges 1000~1300 ms and 30~60, respectively. Because of the same reason, other crucial parameters, such as parallel imaging acceleration factor, NEX, or presence of interpolation, could not be changed.

Receiver BW is known to cause image blurring and affect image quality. A recent study using 3.0T knee MRI and an isotropic 3D-FSE sequence with rBW of 31.25 kHz showed improved image quality but also increased image blurring¹⁵. However, in the present study, rBW was set at 50 kHz and was not changed because a significant increase in image blurring and insufficient fat suppression on FS imaging was noted at a rBW of 35.71 kHz.

Several previous papers have listed the lack of research on the diagnostic performance of isotropic 3D-FSE-Cube-NFS imaging in knee MRI as a study limitation; however, no previous study has compared the diagnostic performance of FS and NFS imaging. Therefore, this study dealt with the core

keyword “without fat suppression.” I wondered if isotropic 3D-FSE-Cube-NFS imaging might show higher diagnostic performance than 3D-FSE-Cube-FS imaging in some clinical situations, including ligament injury, meniscus tear, BME lesion, or cartilage defect. This might be attributed to my line of thought that the low signal intensity of ligaments or menisci and high signal intensity of adjacent fat might contribute to better tissue contrast in NFS imaging than in FS imaging. However, the results of this study show that compared to 3D-FSE-Cube-FS, 3D-FSE-Cube-NFS had similar or inferior diagnostic performance in all clinical settings. I think the main reason for this finding is the lack of tissue contrast increase due to the formation of a fluid signal in the ligament or meniscus when a pathologic lesion appears. Representatively, in the case of MCL tears, a signal increase in the surrounding soft tissue is useful for diagnosing the tear, except for the blurring or discontinuity of the ligament itself. Nevertheless, signal abnormality in the surrounding soft tissue is poorly visible in the NFS images, and hence, 3D-FSE-Cube-NFS showed much lower sensitivity for the detection of MCL tears ($p < 0.001$) (Fig. 5).

The review of 17 cases of MM tears in this study proved the utility of 3D-FSE-Cube-NFS imaging at diagnosing MM tears, because both the readers showed high accuracy of more than 80%. However, compared to FS imaging, NFS imaging had p-values for sensitivity and specificity between 0.05 and 0.1 for the diagnosis of MM tears or cartilage defect lesions. I think there is a strong possibility that a future study on a larger group will show statistically

significant differences.

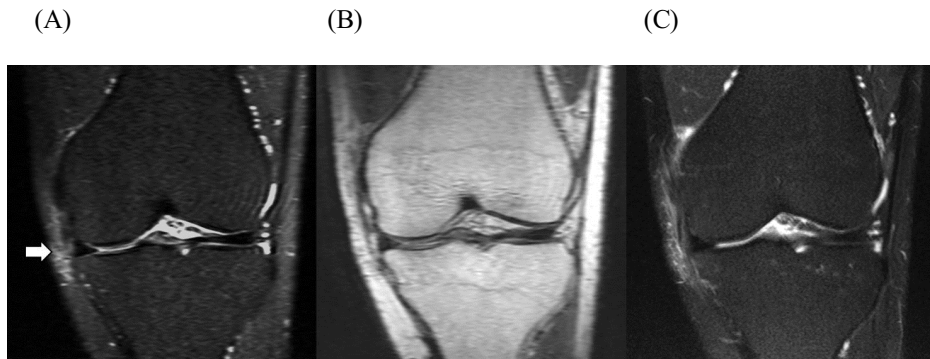


Figure 5. (A) Blurring of the MCL fibers and an increase in the signal intensity of surrounding soft tissue are seen on the coronal reformatted 3D-FSE-Cube-FS image (arrow). (B) Blurring of the ligament fiber is not definite and no signal abnormality in the surrounding soft tissue is detected on the coronal reformatted 3D-FSE-Cube-NFS image. (C) Conventional 2D coronal T2-weighted image reveals the MCL tear.

Based on the arthroscopic surgical findings of 25 patients, 3D-FSE-Cube-FS and 3D-FSE-Cube-NFS imaging sequences have similar diagnostic accuracy for the detection of ACL tears, MM tears, LM tears, and cartilage lesions. Judging from this result, it is possible that 3D-FSE-Cube-NFS can replace 3D-FSE-Cube-FS imaging for the detection of such pathologies. However, the analysis of images of all 124 patients who underwent knee MRI shows different results regarding MCL tears or BME lesions, suggesting that

3D-FSE-Cube-NFS imaging might not to be able to replace 3D-FSE-Cube-FS imaging in those clinical situations. In particular, for subchondral BME lesions, relatively more false-positive cases (61 false-positive segments in all 1078 negative segments) were noted because of subchondral sclerosis or cortical irregularity mimicking BME lesions (Fig. 6).

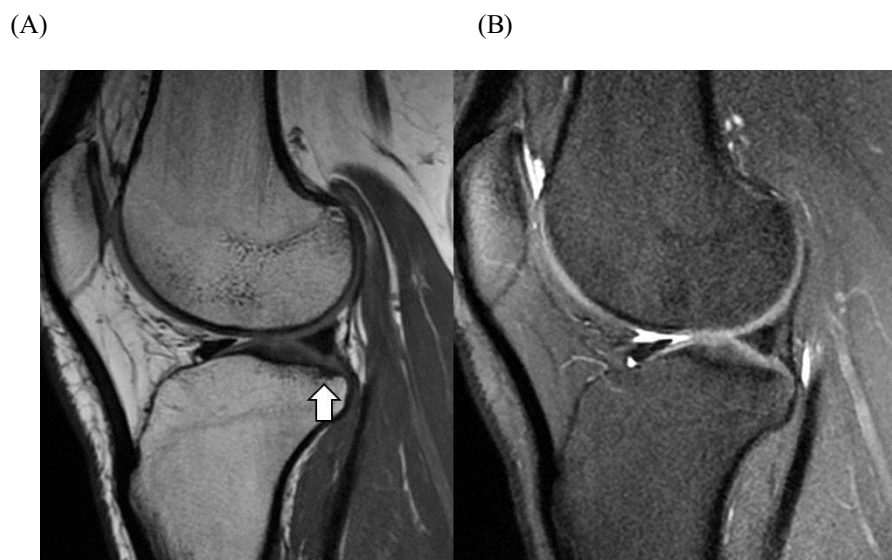


Figure 6. (A) A 3D-FSE-Cube-NFS image showing a suspicious subchondral BME lesion on the posterolateral tibial plateau (arrow). (B) However, in the 3D-FSE-Cube-FS image, a subchondral sclerotic change is seen. After correlation with 2D imaging, it turned out a false-positive lesion.

Although 3D-FSE-Cube-NFS imaging was not superior to 3D-FSE-Cube-FS imaging with statistical significance in all clinical settings, there were some advantages to the additionally obtained 3D-FSE-Cube-NFS sequence during the radiologic reading practice (Figs. 7~9).

First, if the patient's knee had a surgical prosthesis, NFS images showed a relatively weaker susceptibility artifact (Fig. 7). For comparing the severity of artifacts, maximal areas of the metal artifact posterior to the proximal tibial cortex in each sagittal image were measured and compared between FS and NFS images. Two of the 124 patients had previously undergone ACL reconstruction surgery. The average values of maximal area of the metal artifact applied to these patients' images were 95.51 cm² in 3D-FSE-Cube-FS imaging and 53.07 cm² in 3D-FSE-Cube-NFS imaging. Although this topic is not mainly considered in my study because of a small postoperative patient group, this result suggests the possibility that 3D-FSE-Cube-NFS could be more useful than 3D-FSE-Cube-FS imaging in patients with a surgical prosthesis.

Second, 3D-FSE-Cube-NFS images could be more helpful than I thought if there was patient movement during prior 3D-FSE-Cube-FS imaging (Fig. 8). Therefore, the acquisition of an additional 3D-FSE-Cube-NFS image might sometimes lead to a more accurate diagnosis of knee lesions, which might not have been possible using only the 3D-FSE-Cube-FS image.

Third, some cases of subtle BME lesions could be more definitely visible on 3D-FSE-Cube-NFS imaging than on 3D-FSE-Cube-FS imaging (Fig.

9). The reason for this is not yet clear, so further research is warranted in the future. Nevertheless, such cases were not frequent enough to be statistically significant.

Because of these advantages of 3D-FSE-Cube-NFS over 3D-FSE-Cube-FS, future studies should further explore the diagnostic value of adding 3D-FSE-Cube-NFS images to the routine knee MRI protocol.

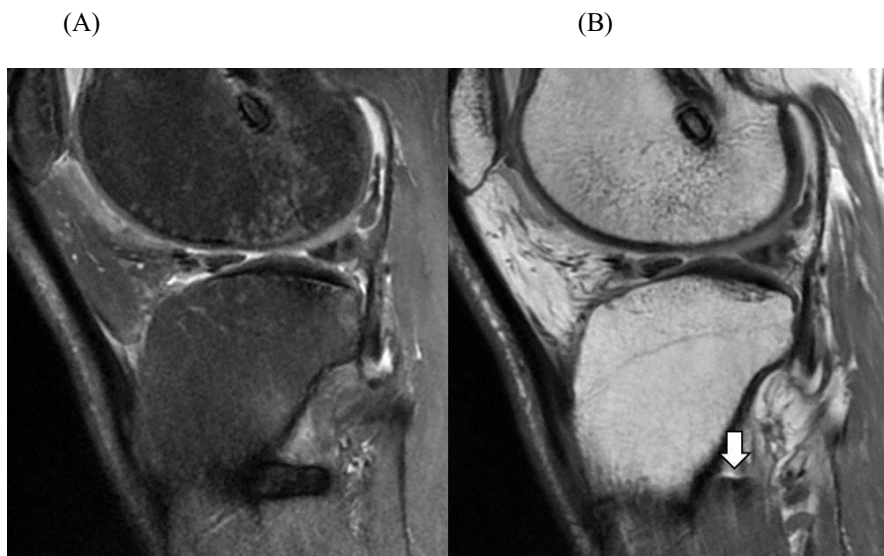


Figure 7. (A) Metal artifact posterior to the proximal tibial cortex in the 3D-FSE-Cube-FS image. (B) Greatly reduced artifact is noted in the 3D-FSE-Cube-NFS image (arrow). The posterior tibial cortex margin is well demarcated in this sequence.

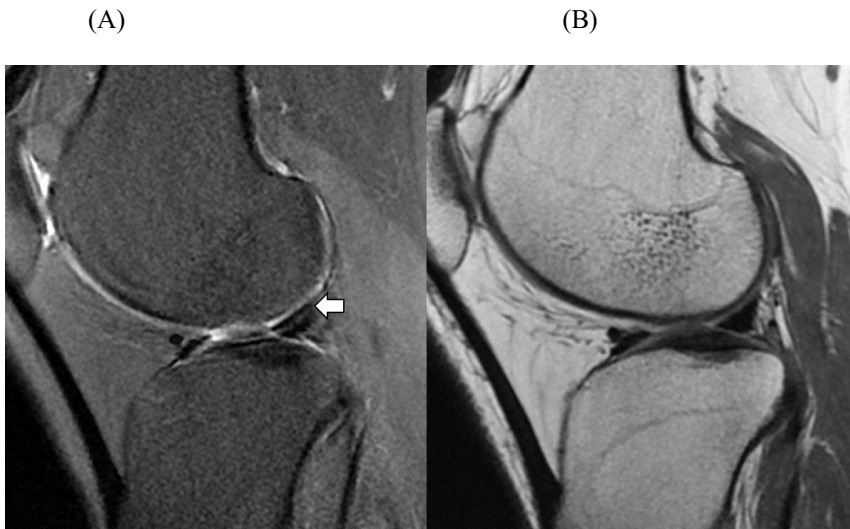


Figure 8. (A) Motion artifact that developed during 3D-FSE-Cube-FS imaging. It is impossible to know whether there is a tear in the LM (arrow). (B) Subsequent 3D-FSE-Cube-NFS image shows a normal meniscus.

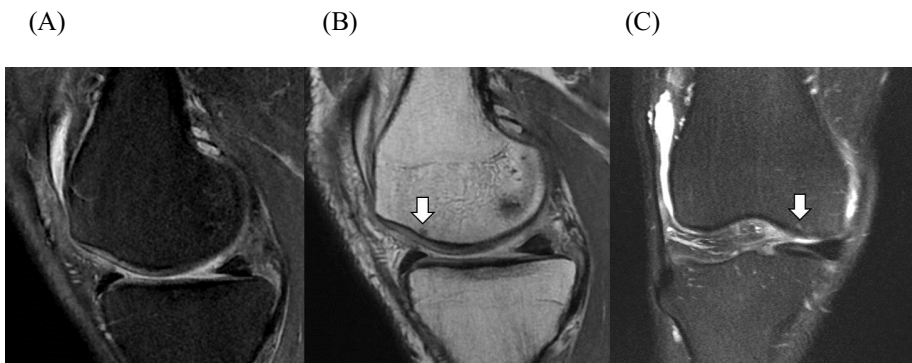


Figure 9. (A) No definite subchondral bone marrow signal change is seen in the medial femoral condyle in the 3D-FSE-Cube-FS image. (B) A small suspicious low signal intensity lesion is seen in the subsequent

3D-FSE-Cube-NFS image (arrow). (C) Conventional 2D coronal T2-weighted image reveals a tiny subchondral BME lesion in the medial femoral condyle (arrow).

The limitations of this study are as follows. First, because there are many possible differences in default parameter settings between my hospital and other institutions, it may not be appropriate for them to apply the optimized scan parameters from this study. However, my result could be utilized as reference or default parameters before specific optimization. Moreover, my optimization methodology can be applied for MR image quality control. Second, during the optimization study, only two parameters (TR and ETL) were changed because of the limits on scan time in a hospital setting. These parameters are basic parameters of image signal intensity and scan time. Third, because of the abovementioned reason, I also set upper and lower limits on TR and ETL; hence, values beyond the limits were not examined. Fourth, because the readers are more familiar with FS images, there is a possibility of relative underestimation of the diagnostic accuracy of the less familiar 3D-FSE-Cube-NFS images. This could be the reason behind the inferior scores of diagnostic performance and interobserver agreements of 3D-FSE-Cube-NFS images. Fifth, because of the small patient group, evaluation of PCL or LCL tears could not be performed. Sixth, because only a few patients with surgical prosthesis of the knee were included, the advantages of NFS imaging in this patient group were not

statistically investigated. This limitation from the small size of the study group can be overcome through further studies on a larger group. Seventh, this study was conducted using only a 1.5T MRI system, but results could be different with a 3.0T MRI system. Further studies using a 3.0T MRI system are needed in the future.

V. Conclusion

In conclusion, considering both acceptable image quality and short scan time, optimized scan parameters for both 3D-FSE-Cube FS and 3D-FSE-Cube NFS were TR=1300 ms and ETL=45. Compared to 3D-FSE-Cube-FS, 3D-FSE-Cube-NFS showed similar sensitivity and specificity for the detection of meniscus tears or cartilage defects, lower sensitivity for the detection of MCL tears, and lower sensitivity and specificity for the detection of BME lesions. In some clinical situations, additional 3D-FSE-Cube-NFS has considerable advantages such as reduced susceptibility artifact, ability for replacing inappropriate 3D-FSE-Cube-FS images, and detection of subtle BME lesions.

References

1. Mackenzie R, Dixon AK, Keene GS, Hollingworth W, Lomas DJ, Villar RN. Magnetic resonance imaging of the knee: assessment of effectiveness. *Clin Radiol* 1996;51:245-50.
2. Gold GE, Busse RF, Beehler C, Han E, Brau AC, Beatty PJ, et al. Isotropic MRI of the knee with 3D fast spin-echo extended echo-train acquisition (XETA): initial experience. *AJR Am J Roentgenol* 2007;188:1287-93.
3. Kijowski R, Blankenbaker DG, Woods M, Del Rio AM, De Smet AA, Reeder SB. Clinical usefulness of adding 3D cartilage imaging sequences to a routine knee MR protocol. *AJR Am J Roentgenol* 2011;196:159-67.
4. Kijowski R, Davis KW, Woods MA, Lindstrom MJ, De Smet AA, Gold GE, et al. Knee joint: comprehensive assessment with 3D isotropic resolution fast spin-echo MR imaging--diagnostic performance compared with that of conventional MR imaging at 3.0 T. *Radiology* 2009;252:486-95.
5. Jung J-Y, Jee W-H, Park MY, Lee S-Y, Kim J-M. Meniscal tear configurations: categorization with 3D isotropic turbo spin-echo MRI compared with conventional MRI at 3 T. *American Journal of Roentgenology* 2012;198:W173-W80.

6. Jung JY, Yoon YC, Kim HR, Choe BK, Wang JH, Jung JY. Knee derangements: comparison of isotropic 3D fast spin-echo, isotropic 3D balanced fast field-echo, and conventional 2D fast spin-echo MR imaging. *Radiology* 2013;268:802-13.
7. Jung JY, Yoon YC, Kwon JW, Ahn JH, Choe B-K. Diagnosis of Internal Derangement of the Knee at 3.0-T MR Imaging: 3D Isotropic Intermediate-weighted versus 2D Sequences 1. *Radiology* 2009;253:780-7.
8. Lim D, Han Lee Y, Kim S, Song HT, Suh JS. Clinical value of fat-suppressed 3D volume isotropic spin-echo (VISTA) sequence compared to 2D sequence in evaluating internal structures of the knee. *Acta Radiol* 2016;57:66-73.
9. Ai T, Zhang W, Priddy NK, Li X. Diagnostic performance of CUBE MRI sequences of the knee compared with conventional MRI. *Clin Radiol* 2012;67:e58-63.
10. Kijowski R, Davis KW, Blankenbaker DG, Woods MA, Del Rio AM, De Smet AA. Evaluation of the menisci of the knee joint using three-dimensional isotropic resolution fast spin-echo imaging: diagnostic performance in 250 patients with surgical correlation. *Skeletal Radiol* 2012;41:169-78.
11. Ristow O, Steinbach L, Sabo G, Krug R, Huber M, Rauscher I, et al. Isotropic 3D fast spin-echo imaging versus standard 2D imaging at 3.0

- T of the knee—image quality and diagnostic performance. *European radiology* 2009;19:1263-72.
12. Duc SR, Pfirrmann CW, Koch PP, Zanetti M, Hodler J. Internal Knee Derangement Assessed with 3-minute Three-dimensional Isovoxel True FISP MR Sequence: Preliminary Study 1. *Radiology* 2008;246:526-35.
 13. Lim D, Lee YH, Kim S, Song H-T, Suh J-S. Fat-suppressed volume isotropic turbo spin echo acquisition (VISTA) MR imaging in evaluating radial and root tears of the meniscus: focusing on reader-defined axial reconstruction. *European journal of radiology* 2013;82:2296-302.
 14. Chen CA, Kijowski R, Shapiro LM, Tuite MJ, Davis KW, Klaers JL, et al. Cartilage morphology at 3.0T: assessment of three-dimensional magnetic resonance imaging techniques. *J Magn Reson Imaging* 2010;32:173-83.
 15. Li CQ, Chen W, Rosenberg JK, Beatty PJ, Kijowski R, Hargreaves BA, et al. Optimizing isotropic three-dimensional fast spin-echo methods for imaging the knee. *J Magn Reson Imaging* 2014;39:1417-25.
 16. Delfaut EM, Beltran J, Johnson G, Rousseau J, Marchandise X, Cotten A. Fat suppression in MR imaging: techniques and pitfalls. *Radiographics* 1999;19:373-82.
 17. Cho KE, Yoon C-S, Song H-T, Lee YH, Lim D, Suh J-S, et al. Quantitative Assessment and Ligament Traceability of Volume Isotropic

- Turbo Spin Echo Acquisition (VISTA) Ankle Magnetic Resonance Imaging: Fat Suppression versus without Fat Suppression. *Journal of the Korean Society of Magnetic Resonance in Medicine* 2013;17:110-22.
18. De Smet AA, Norris MA, Yandow DR, Quintana FA, Graf BK, Keene JS. MR diagnosis of meniscal tears of the knee: importance of high signal in the meniscus that extends to the surface. *AJR Am J Roentgenol* 1993;161:101-7.
 19. De Smet AA, Tuite MJ, Norris MA, Swan JS. MR diagnosis of meniscal tears: analysis of causes of errors. *AJR Am J Roentgenol* 1994;163:1419-23.
 20. Bredella MA, Tirman PF, Peterfy CG, Zarlingo M, Feller JF, Bost FW, et al. Accuracy of T2-weighted fast spin-echo MR imaging with fat saturation in detecting cartilage defects in the knee: comparison with arthroscopy in 130 patients. *AJR Am J Roentgenol* 1999;172:1073-80.
 21. Potter HG, Linklater JM, Allen AA, Hamafin JA, Haas SB. Magnetic resonance imaging of articular cartilage in the knee. An evaluation with use of fast-spin-echo imaging. *J Bone Joint Surg Am* 1998;80:1276-84.
 22. Sonin AH, Pensy RA, Mulligan ME, Hatem S. Grading articular cartilage of the knee using fast spin-echo proton density-weighted MR imaging without fat suppression. *AJR Am J Roentgenol* 2002;179:1159-66.

23. Noyes FR, Stabler CL. A system for grading articular cartilage lesions at arthroscopy. *The American Journal of Sports Medicine* 1989;17:505-13.
24. Seigel DG, Podgo MJ, Remaley NA. Acceptable values of kappa for comparison of two groups. *American journal of epidemiology* 1992;135:571-8.

ABSTRACT (IN KOREAN)

무릎 관절에서 지방신호억제를 하지 않은 등방성 3차원
고속스핀에코 영상: 1.5T MRI에서의 영상 파라미터 최적화 및
지방신호억제 영상과의 진단 정확도 비교

<지도교수 서진석>

연세대학교 대학원 의학과

조희우

배경 및 목적: 자기공명 영상에서 가변 플립각 (flip angle) 을 이용하는 3 차원 고속스핀에코 (fast spin echo, FSE) 영상은 등방성 영상 재구성이 가능하여, 무릎 자기공명 영상 기본 프로토콜의 필수적인 시퀀스에 포함되어 사용되고 있다.

지방억제를 적용하여 시행한 가변 플립각 3 차원 고속스핀에코 (지방억제) 영상과 적용하지 않은 (비지방억제) 영상의 비교는 이전에 연구되지 않았으며, 비지방억제 등방성 3 차원 고속스핀에코 영상의 진단적 유용성은 알려진 바 없다. 이 연구의 목적은 (1) 1.5T 무릎 자기공명영상에서 지방억제 및

비지방억제 등방성 3 차원 고속스핀에코 영상의 촬영 파라미터 최적화하고, (2) 무릎 내 반월판, 인대, 골수 및 연골의 병변의 발견에 있어서 비지방억제 등방성 3 차원 고속스핀에코 영상의 진단적 유용성을 지방억제 영상과의 비교를 통해 평가하는 것이다.

방법: 돼지 무릎 팬텀을 이용하여 1.5T MRI (Signa Horizon; GE Healthcare, Waukesha, WI, USA) 에서 지방억제 및 비지방억제 등방성 3 차원 고속스핀에코 영상의 촬영 파라미터를 최적화하였다. 이를 위해 1000 ms 에서 1300 ms 까지 repetition time (TR) 과 30 에서 60 까지 echo train length (ETL) 를 다양하게 조합한 시상면 영상을 얻었다. TR=1300 ms 그리고 ETL=30 인 영상이 기준 영상으로 설정되었다. 두 명의 근골격계 영상의학과 전문의들이 기준 영상을 레퍼런스로 하여 각각의 팬텀 영상들을 대상으로 영상의 흐릿한 정도와 전체적인 영상의 질에 대해 -8 점에서 8 점까지 범위의 점수로 평가하였다. 그 후 팬텀 연구에서 -2 점 또는 그 이상의 점수를 얻은 파라미터 조합의 영상들을 건강한 지원자를 대상으로 얻어 *in vivo* 영상을 얻어, 같은 방식으로 평가하였다. 각 영상마다 슬개골 연골과 대퇴골 골수에서 신호대잡음비 (signal to noise ratio, SNR) 와 단위시간당 신호대잡음비 (SNR/unit time) 를

구하였다. 영상의학과 전문의들의 영상 질 평가와 단위시간당 신호대잡음비를 모두 고려하여 최적화된 촬영 파라미터를 결정하였다. 최적화된 파라미터를 적용하여 2015년 9월부터 같은 해 12월까지 총 124명의 무릎 통증 환자들을 대상으로 지방억제 및 비지방억제 등방성 3차원 고속스핀에코 영상을 포함한 무릎 관절 MRI를 촬영하였다. 그들 중 25명은 MRI 촬영 이후 관절경 수술을 시행받았다. 관절경 수술 소견과 2차원 영상들을 표준지표로 하여 2명의 영상의학과 전문의들이 지방억제와 비지방억제 등방성 3차원 고속스핀에코 영상의 진단적 유용성을 비교하여 인대 파열, 반월판 파열, 연골하골수부종 또는 연골 결손과 같은 상황에 대한 영상의학적 진단에서 어느 영상이 더 진단적인지를 평가하였다. 두 영상의 진단적 유용성을 통계적으로 비교하기 위하여 McNemar's test를 이용하였고 $p < 0.05$ 일 경우 통계적으로 유의미한 것으로 보았다.

결과: 영상 질과 신호대잡음비는 TR이 크고 ETL이 작을수록 증가하였다. -1 점 이상의 점수를 얻은 팬텀 영상들 중에서 가장 높은 단위시간당 신호대잡음비를 보인 최적화된 촬영 파라미터 조합은 지방억제 및 비지방억제 영상에서 모두 TR=1300 ms 그리고 ETL 45였다. 건강한 지원자 영상에서도 같은 파라미터

조합이 지방억제 및 비지방억제 영상에서 모두 최적으로 판정되었다. 124 명의 환자 영상에서, 비지방억제 등방성 3차원 고속스핀에코 영상은 내측인대 파열과 골수부종 병변을 제외하고 반월판 파열과 연골 결손에 있어서는 지방억제 등방성 3차원 고속스핀에코 영상에 비하여 비슷한 진단적 유용성을 보였다. 다만 내측 인대 파열의 발견에서는 낮은 민감도를, 골수부종 병변의 발견에서는 낮은 민감도와 낮은 특이도를 보였다. 비지방억제 등방성 3차원 고속스핀에코 영상은 자화 감수성 인공물이 적고, 부적절하게 촬영된 지방억제 등방성 3차원 고속스핀에코 영상을 대체할 수 있으며, 미세한 골수부종 병변을 때때로 더 잘 발견할 수 있는 등 상당한 장점을 보였다.

결론: 적절한 영상의 질과 최대한 짧은 촬영 시간을 함께 고려하였을 때 최적의 촬영 파라미터는 지방억제 및 비지방억제 등방성 3차원 고속스핀에코 영상에서 모두 TR=1300 ms 그리고 ETL=45의 조합이었다. 지방억제 등방성 3차원 고속스핀에코 영상과 비교하였을 때 비지방억제 등방성 3차원 고속스핀에코 영상은 반월판 파열이나 연골 결손에 있어서는 비슷한 민감도와 특이도를 보였고, 내측인대 파열에 대해서는 낮은 민감도를, 골수부종 병변에 대해서는 낮은 민감도와 특이도를 보였다. 추가적인 비지방억제 등방성 3차원

고속스핀에코 영상은 자화 감수성 인공물이 적은 등 여러 장점이 있어, 특정한 임상적 상황에서는 부적절한 지방억제 등방성 3차원 고속스핀에코 영상을 대체할 수 있는 선택지가 될 수 있다.

핵심되는 말 : 무릎, 자기공명영상, 3차원, 지방억제